Journal of Power Sources 189 (2009) 435–439

Contents lists available at ScienceDirect

Journal of Power Sources

journal homepage: www.elsevier.com/locate/jpowsour

Short communication

Electrochemical properties of $LiFe_{0.9}Mn_{0.1}PO_4/Fe_2P$ cathode material by mechanical alloying

Kyung Tae Lee [a,b,*], Kyung Sub Lee [a]

[a] Department of Materials Science & Engineering, Hanyang University, Seoul 133-791, Republic of Korea
[b] Umicore Korea Limited, 410, Chaam-dong, Cheonan-city, 330-200, Republic of Korea

ARTICLE INFO

Article history:
Received 16 June 2008
Received in revised form
28 November 2008
Accepted 22 December 2008
Available online 30 December 2008

Keywords:
$LiFePO_4$
Fe_2P
Mechanical alloying
$LiFeMnPO_4$
Cathode material

ABSTRACT

$LiFePO_4$, olivine-type $LiFe_{0.9}Mn_{0.1}PO_4/Fe_2P$ composite was synthesized by mechanical alloying of carbon (acetylene back), M_2O_3 (M = Fe, Mn) and $LiOH{\cdot}H_2O$ for 2 h followed by a short-time firing at 900 °C for only 30 min. By varying the carbon excess different amounts of Fe_2P second phase was achieved. The short firing time prevented grain growth, improving the high-rate charge/discharge capacity. The electrochemical performance was tested at various *C*/*x*-rate. The discharge capacity at 1*C* rate was increased up to 120 mAh g^{-1} for the $LiFe_{0.9}Mn_{0.1}PO_4/Fe_2P$ composite, while that of the unsubstituted $LiFePO_4/Fe_2P$ and $LiFePO_4$ showed only 110 and 60 mAh g^{-1}, respectively. Electronic conductivity and ionic diffusion constant were measured. The $LiFe_{0.9}Mn_{0.1}PO_4/Fe_2P$ composite showed higher conductivity and the highest diffusion coefficient (3.90×10^{-14} cm^2 s^{-1}). Thus the improvement of the electrochemical performance can be attributed to (1) higher electronic conductivity by the formation of conductive Fe_2P together with (2) an increase of Li^+ ion mobility obtained by the substitution of Mn^{2+} for Fe^{2+}.

1. Introduction

Because of its low cost, low toxicity and high safety Lithium iron phosphate is attractive as cathode material in lithium rechargeable battery [1–4]. A main challenge to implement $LiFePO_4$ is the intrinsically poor rate capability caused by low electronic conductivity and comparable low Li-ion diffusion [5,6].

Several approaches are known to improve the electronic conductivity of $LiFePO_4$: Carbon coating [7–9], super-valent ion doping [5,10–13], grain refinement [14–16] and the creation of electronic conductive metal-rich phosphide [17]. The phosphides form as second phase under reducing atmosphere at high temperature [17].

$LiFePO_4$ has been synthesized by a variety of routes. The authors focus on the carbothermal reduction (CTR) method, introduced by Baker et al. [18]. In this method three valent Fe_2O_3 and carbon (acting as reducing agent) are used as precursors. Compared with other methods which use divalent iron precursors like iron acetate or iron oxalate, the CTR method is more easy to scale-up: first, Fe_2O_3 is cheaper, and second, during firing it forms much less hazardous gas.

In a previous study [19], the authors applied the CTR method together with mechanical alloying (MA) using excess carbon and firing at high temperature. Similar approaches to improve the conductivity of $LiFePO_4$ have been reported by Nazar and co-workers [17] and Xu et al. [20]. This method allows achieving a $LiFePO_4/Fe_2P$ composite-network with higher electronic conductivity. In case of 3 wt% of excess carbon good electrochemical properties were achieved. Compared to the $LiFePO_4$ reference (10^{-9} S cm^{-1}) the electronic conductivity of the $LiFePO_4/Fe_2P$ composite increased to 10^{-3} to 10^{-1} S cm^{-1}.

To achieve good electrochemical performance requires not only a high electronic conductivity but also a fast ionic transport; corresponding to a high Li^+ solid state diffusion coefficient. The authors believe that the substitution of Mn for Fe – due to the larger ionic radius of Mn^{2+} – facilitates a wider channel for Li diffusion which enhances the mobility of the Li ion. Therefore in the actual study the authors focus on manganese substituted $LiFePO_4$. (At the same time it is fused on $LiMPO_4/Fe_2P$ composites to achieve high electronic conductivity.) 10% substitution (M = $Fe_{0.9}Mn_{0.1}$) was chosen. We chose 10% because if the number is much smaller we expect very little change whereas if the number is larger we observe the two-step voltage plateau which might cause problems in battery applications. Finally, good electrochemical performance requires a short solid state diffusion path, so the authors focus on small particles within the composite. These smaller particles are achieved by short-time firing preventing excessive sintering.

The present study evaluates the morphology and phase composition of $LiMPO_4/Fe_2P$ composite powders with 10% Mn^{2+}. The study reports the conductivity and Li^+ diffusion coefficient as well as the charge/discharge capacity. The results are compared with

* Corresponding author. Tel.: +82 2 2281 4914; fax: +82 2 2281 4914.
E-mail address: lkt0912@naver.com (K.T. Lee).

0378-7753/$ – see front matter.
doi:10.1016/j.jpowsour.2008.12.090

those of unsubstituted $LiFePO_2/Fe_2P$ composites and with single phase $LiFePO_4$.

Naming: For simplicity we will refer to a 10% Mn substituted composite sample as $LiFe_{0.9}Mn_{0.1}PO_4/Fe_2P$ composite despite that the accurate formula for M in the $LiMPO_4/Fe_2P$ might be slightly different.

2. Experimental

The $LiFe_{0.9}Mn_{0.1}PO_4/Fe_2P$ composite samples were prepared by the mechanical alloying (MA) process with carbon excess. As starting materials $LiOH{\cdot}H_2O$ (Aldrich, ≥98%), Fe_2O_3 (Aldrich, ≥99%), $(NH_4)_2{\cdot}HPO_4$ (Aldrich, ≥99%), Mn_2O_3 (Aldrich ≥99%) and acetylene black powders were used. The metal composition was either 100% Fe_2O_3 or 90% Fe_2O and 10% Mn_2O_3. The stoichiometric amount of carbon is 1/2 mol per 1 mol of Fe + Mn. The carbon excess was either 0, 3, 5, 7 wt%, relative to the stoichiometric amount.

The MA process was carried out for 2 h under an argon atmosphere using a shaker type of ball mill (SPEX 8000 M) that rotated at around 1000–1050 rpm. The ball to powder mass ratio was 15, and 1/2 in. (≅12.5 mm balls) steel balls were used. The ball-milled powders were fired at 900 °C. Firing time was varied from 5 h to 30 min in a tube-type vacuum furnace. The heating and cooling ramp was 30 K min^{-1}. More details have been reported elsewhere [19].

The powder morphology and particle size of the $LiMPO_4/Fe_2P$ composites were investigated by means of field emission scanning electron microscopy (FE-SEM). The structure was investigated by XRD (Rigaku D-MAX 3000) using Cu Kα radiation (2θ scanning range: 15°–130°, step-size: 0.02°, step time: 8 s). Unit cell parameters of the main $LiMPO_4$ phase and the quantitative ratio of $LiMPO_4$ and Fe_2P phase was obtained from a Rietveld refinement. The general structure analysis system (GSAS) program was used. As profile function, Pseudo-Voight function was chosen.

The electronic conductivity of pressed pellets was measured by using a four-point probe (Advanced Instrument Technology, CMT-SR3000). Electrochemical characterization of the $LiFePO_4/Fe_2P$ and $LiFe_{0.9}Mn_{0.1}PO_4/Fe_2P$ cathode material was carried out using two-electrode half-cells as described in the previous work [21].

The diffusion coefficient of Li ion was measured by GITT (galvanostatic intermittent titration technique) using three-electrode beaker cells. Current pulses of 0.25 mA were applied for 1800 s and the voltage response was monitored. After the pulse a rest of 1800 s followed. As working electrodes, punched disks with 1 cm^2 area was used, the active loading was approx. 20 mg. Ethylene carbonate(EC)/dimethyl carbonate(DMC) (1:1 by volume) with 1 M $LiPF_6$ was used as electrolyte. The theoretical background of using GITT for $LiFePO_4$ is in detail described in the literature [22]. Our analysis follows the procedures given in the paper.

The cells were cycled using an automatic galvanostatic charge–discharge unit (Maccor 4000 series) at various *C* rates, between 2.5 and 4.3 V at ambient temperature (25 ± 2 °C).

3. Results and discussion

As a result of detailed DTA, DSC and TGA studies the authors propose the following reaction mechanism of the ball-milled precursor blends during firing:

$$LiOH{\cdot}H_2O \rightarrow LiOH + H_2O(\text{at}50\text{–}130\,^\circ\text{C}) \quad (1)$$

$$(NH_4)_2H{\cdot}PO_4 \rightarrow 2(NH)_3 + H_3PO_4(\text{at}130\text{–}200\,^\circ\text{C}) \quad (2)$$

$$LiOH + H_3PO_4 \rightarrow LiH_2PO_4 + H_2O(\text{at}200\text{–}480\,^\circ\text{C}) \quad (3)$$

$$LiH_2PO_4 + 0.5Fe_2O_3 + 0.5C \rightarrow LiFePO_4 + H_2O + 0.5CO(\text{at}480\text{–}900\,^\circ\text{C}) \quad (4)$$

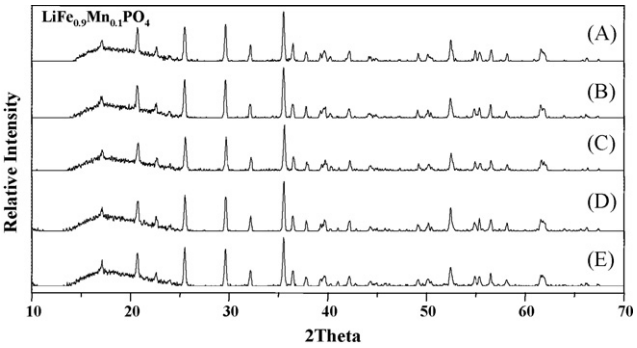

Fig. 1. X-ray diffraction pattern of $LiFe_{0.9}Mn_{0.1}PO_4$ samples after 900 °C firing temperature with various annealing time. (A) 30 min, (B) 1 h, (C) 2 h, (D) 3 h and (E) 5 h.

$$(\text{Combined})LiOH{\cdot}H_2O + 0.5(Fe_2O_3) + (NH_4)_2H{\cdot}PO4 + 0.5C \rightarrow LiFePO_4 + 3H_2O + 2(NH_3) + 0.5CO$$

First, we will discuss X-ray and FE-SEM results of a series of samples which investigate shorter firing times to obtain less sintered (smaller) particles. The issues are (1) if short firing time is sufficient to complete the reaction and (2) if smaller particles are obtained? All samples were prepared without excess of carbon, aiming at a one-phase $LiMPO_4$. The firing time was varied from 5 h to 30 min at 900 °C.

Fig. 1 shows the X-ray diffraction pattern for $LiFe_{0.9}Mn_{0.1}PO_4$ for various firing times (5 h, 3 h, 2 h, 1 h and 30 min). (A small hump visible at 13°–26° is not related to the sample, but caused by tape used for fixing the small amounts of available sample.) In all cases single phase $LiFe_{0.9}Mn_{0.1}PO_4$ was achieved. It has an ordered olivine structure indexed to the orthorhombic *Pmna* space group. The crystal structure is similar as that of undoped $LiFePO_4$ whereas the unit cell volume slightly confirms successful doping; the Mn^{2+} – which has larger ionic radius (0.97 Å) than Fe^{2+} (0.92 Å) is well dispersed within the $LiFePO_4$ crystal structure.

Fig. 2 shows FE-SEM micrographs of the samples prepared for firing times (10 h, 5 h, 2 h and 30 min). Clearly visible is the effect of prolonged sintering. The grain size increases from approx. 1 μm for 30 min firing to 1.5, 2 and 3 μm for 2, 5, and 10 h firing time, respectively.

The X-ray results showing the increase of lattice relative to $LiFePO_4$ doping together with the FE-SEM confirms that the short-time firing of the ball milled precursor was successful: Already after 30 min small sized and well crystallized homogeneous $LiMPO_4$ particles are achieved.

The 30 min firing-at-high-temperature was applied to prepare $LiMPO_4/Fe_2P$ composite samples by using carbon excess. A series of four samples was prepared: (a) M = Fe and (b) M = $Fe_{0.9}Mn_{0.1}$ having either (i) 3% and (ii) 5% carbon excess, respectively. A reference $LiFePO_4$ (no Mn substitution, no carbon excess) and a reference $LiFe_{0.9}Mn_{0.1}PO_4$ (no carbon excess, 10% Mn substitution) was prepared in a similar manner.

Fig. 3 compares the X-ray diffraction pattern of 10% Manganese substituted samples prepared with 0, 3 and 5% carbon excess. Fig. 4 is the Rietveld refinement for $LiFe_{0.9}Mn_{0.1}PO_4$ and Table 1 summarizes the results of Fig. 4. The Rietveld refinement confirms that samples prepared with *C* excess are composites of $LiMPO_4$ and Fe_2P, whereas the sample without carbon excess is single-phase $LiMPO_4$.

The Rietveld refinement allows to quantitatively estimate the phase ratio. So the content of Fe_2P phase in the $LiFe_{0.9}Mn_{0.1}PO_4/Fe_2P$ composite increases from 4.1% to 7.2% when the carbon excess increases from 3% to 5%.

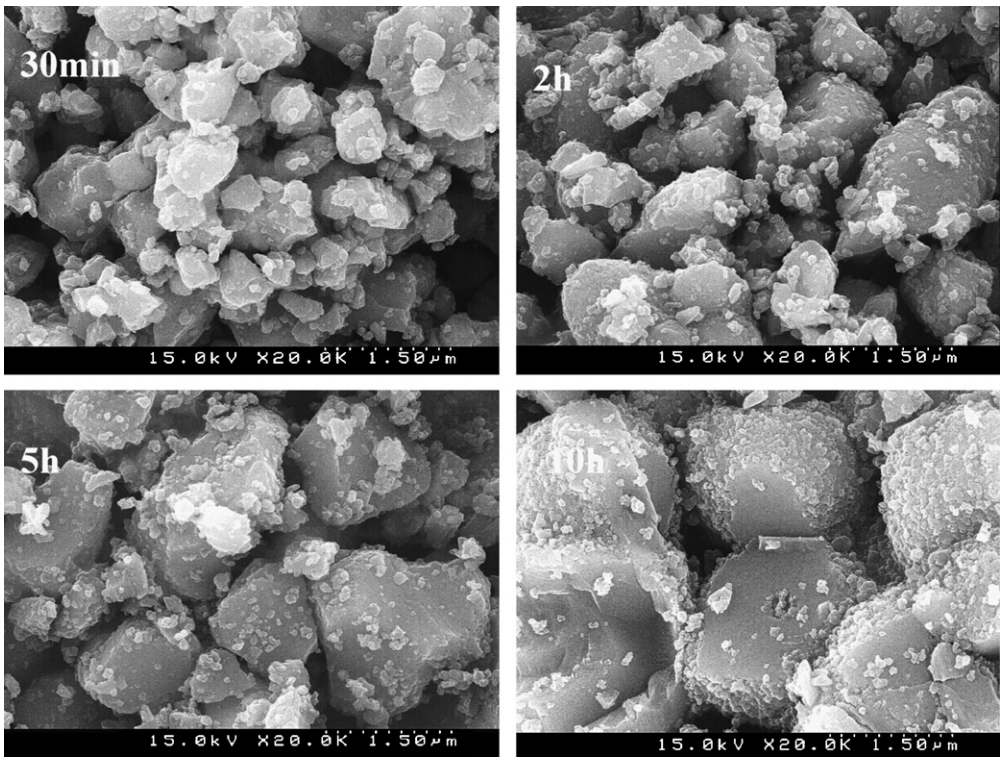

Fig. 2. SEM images of LiFePO4 prepared by MA after firing at 900 °C for various times.

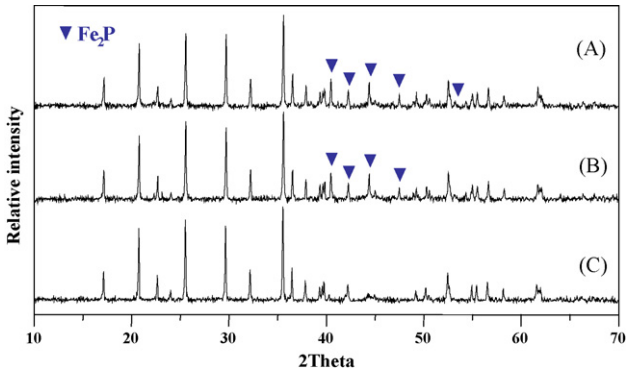

Fig. 3. X-ray diffraction patterns for (A) $LiFe_{0.9}Mn_{0.1}PO_4/Fe_2P$ (excess 5 wt% carbon adding) (B) $LiFe_{0.9}Mn_{0.1}PO_4/Fe_2P$ (excess 3 wt% carbon adding) (C) $LiFe_{0.9}Mn_{0.1}PO_4$.

We aimed at approx. 4% of Fe_2P phase. As shown in our previous paper [19], we expect optimum performance, i.e. high rate and high capacity in this region. If the Fe_2P is much higher the theoretical capacity is low, if the Fe_2P is smaller the electronic conductivity will be low. The 3% carbon excess sample has the target ratio of Fe_2P phase.

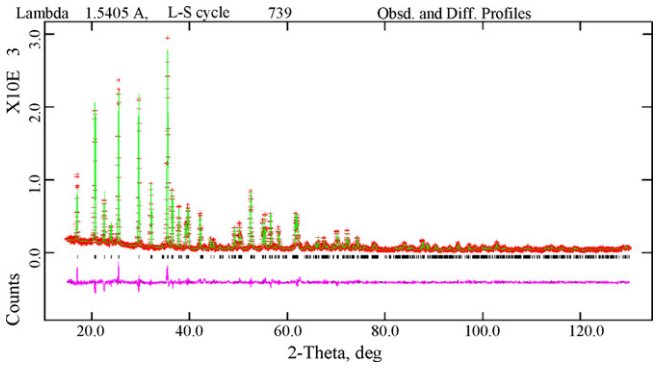

Fig. 4. Rietveld refinement patterns for $LiFe_{0.9}Mn_{0.1}PO_4/Fe_2P$ composite.

Table 1
Lattice parameters and Rietveld coefficients of the prepared samples.

	a (Å)	b (Å)	c (Å)	V (Å^3)	R_{wp}/R_p
$LiFePO_4/Fe_2P$	10.3263	6.0075	4.6917	291.05	1.70
$LiFe_{0.9}Mn_{0.1}PO_4/Fe_2P$	10.3624	6.0342	4.6979	293.75	1.65

In the following we will discuss results of electrochemical testing (electronic conductivity, GITT, coin cell) of the $LiFe_{0.9}Mn_{0.1}PO_4/Fe_2P$ composite sample prepared with 3% carbon excess and compare these results with (1) the $LiFePO_4/Fe_2P$ composite (3% carbon excess), and (2) the $LiFePO_4$ (no carbon excess) reference.

Table 2 shows the results of the electronic conductivity test. The electronic conductivity of the $LiMPO_4/Fe_2P$ composites (both $M = Fe_{0.9}Mn_{0.1}$ and $M = Fe$) have an electronic conductivity which is about 10^4 times higher than that of the $LiFePO_4$ reference.

As discussed before – inorder to obtain a high rate performance – not only good electronic conductivity but also high Li diffusion constant is needed. We measured the diffusion constant by the GITT method; the diffusion coefficient of lithium D was obtained according to Eq. (1) derived by Weppner and Huggins [23]

$$D_{Li} = \frac{4}{\pi}\left(\frac{V_m}{SF}\right)^2 \times \left[\frac{I^o(\delta E/\delta x)}{(\delta E/\delta t^{1/2})}\right]^2 \quad (1)$$

Table 2
Electronic conductivity of the prepared samples.

	Electronic conductivity (S cm^{-1})
$LiFePO_4$	8.20×10^{-8}
$LiFePO_4/Fe_2P$	1.02×10^{-4}
$LiFe_{0.9}Mn_{0.1}PO_4/Fe_2P$	2.72×10^{-4}

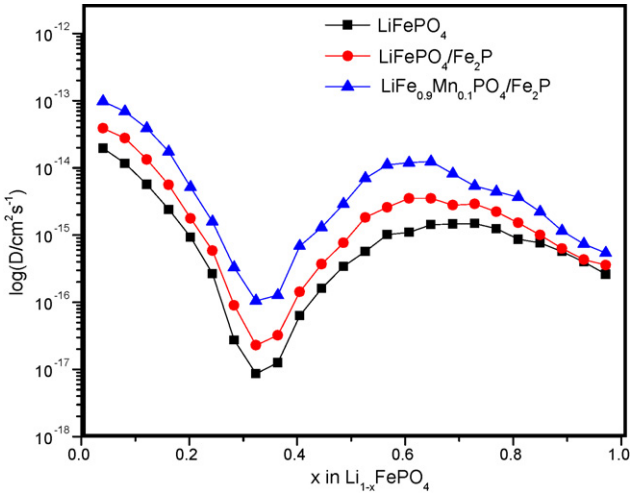

Fig. 5. The plot of the lithium chemical diffusion coefficients obtained by GITT as a function of lithium content x in $Li_{1-x}FePO_4$.

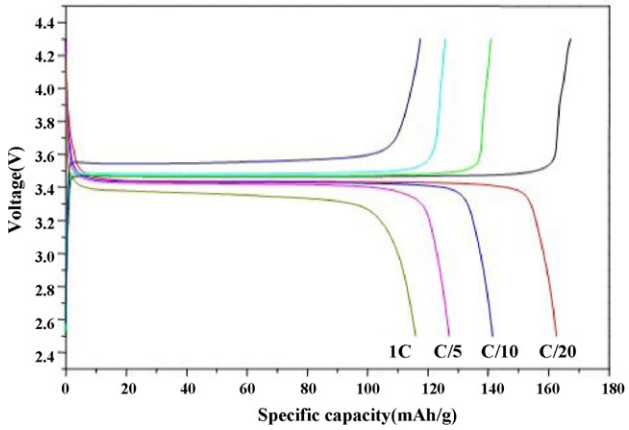

Fig. 6. The charge/discharge profile of capacity of $LiFe_{0.9}Mn_{0.1}PO_4/Fe_2P$ composite (excess 3 wt% carbon adding).

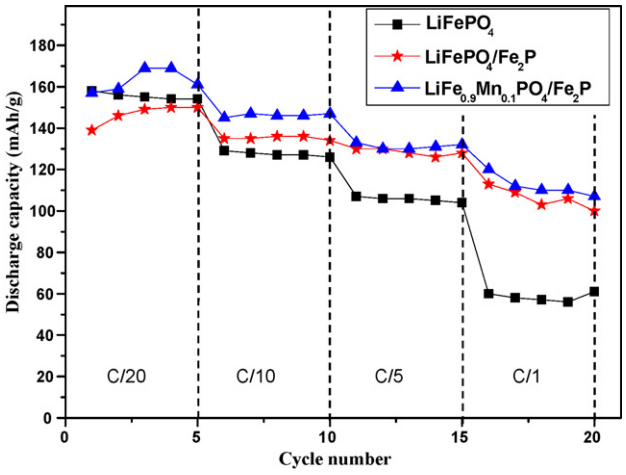

Fig. 7. The Charge/Discharge capacity of $LiFePO_4$, $LiFePO_4/Fe_2P$ and $LiFe_{0.9}Mn_{0.1}PO_4/Fe_2P$. (at $C/20$, $C/10$, $C/5$ and $1C$ rate).

where V_m is the phosphate molar volume (44.11 $cm^3\,mol^{-1}$), S is the contact area between electrolyte and sample (1 cm^2), F is the faraday constant (96,486 C mol^{-1}), I^o is the applied constant electric current (2.5×10^{-4} A), $\delta E/\delta x$ is the slope of the coulometric titration curve while $\delta E/\delta t^{1/2}$ is the slope of the short-time transient voltage change. $\delta E/\delta x$ is obtained from the change of steady state voltage δE after the pulse where δx is the amount of intercalated Li (mol) calculated from the current, active mass and pulse duration of lithium stoichiometry. $\delta E/\delta t^{1/2}$ is the slope of the voltage transient plotted versus $t^{1/2}$ at the beginning of the pulse. Refs. [22,24] give more detailed information. Eq. (1) is valid for times shorter then the diffusion time $\tau = (d/2\pi)^2/D$ where d is the average diameter of the grains.

A paper by Prosini et al. [22] discusses in detail the application of the GITT method to measure diffusion constants for a system like $LiFePO_4$ where – strictly spoken – a diffusion constant does not exist because the intercalation occurs by a moving phase boundary mechanism between the fully intercalated and fully de-intercalated phase. In our analysis we follow the procedures of the paper.

Fig. 5 shows the results for the chemical Li diffusion constant D obtained by the GITT measurement as function of state of charge. Our results for the $LiFePO_4$ reference are remarkable similar to those published in [22]. The curves of the figure show that the value of the chemical diffusion constant varies significantly as function of state of charge. The three samples ($LiFe_{0.9}Mn_{0.1}PO_4/Fe_2P$, $LiFePO_4/Fe_2P$, $LiFePO_4$) show the same general shape – the maximum diffusivity is achieved for $x = 0$ and $x \cong 0.6$ in $Li_{1-x}MPO_4$.

Fig. 5 shows that Li diffusion constant of the 10% Mn substituted composite sample is generally about 1/2 order of magnitude larger than the $LiFePO_4/Fe_2P$ composite which again is higher than the $LiFePO_4$ reference.

The lithium ion diffusion coefficients of the $LiFePO_4$, $LiFePO_4/Fe_2P$ and $LiFe_{0.9}Mn_{0.1}PO_4/Fe_2P$ were measured to be 5.68×10^{-15}, 1.34×10^{-14} and 3.90×10^{-14} $cm^2\,s^{-1}$, respectively. Nakamura et. al [25] has reported a similar trend – a higher diffusion coefficient for a Mn substituted $LiFe_{0.9}Mn_{0.1}PO_4$. The absolute number of diffusion coefficient, however, is different to that obtained in this study.

Fig. 6 shows the charge and discharge voltage profile of the $LiFe_{0.9}Mn_{0.1}PO_4/Fe_2P$ composite. The figure shows that the voltage profile of the $LiFe_{0.9}Mn_{0.1}PO_4/Fe_2P$ composite is about similar to that of $LiFePO_4$ – i.e. we observe a large flat 3.4 V plateau possibly originating from a two-phase equilibrium between fully lithiated $LiMPO_4$ and fully delithiated MPO_4. The discharge capacity was 165 mAh g^{-1} at $C/20$ rate, which is 95% of the theoretical capacity. At $1C$ rate the capacity dropped to 120 mAh g^{-1} about 70% of the theoretical capacity.

Fig. 7 shows the discharge capacity at various rates ($C/20$, $C/10$, $C/5$ and $1C$) as a function of cycle number for the three samples ($LiFe_{0.9}Mn_{0.1}PO_4/Fe_2P$, $LiFePO_4/Fe_2P$, $LiFePO_4$ reference). Single phase $LiFePO_4$ showed 156 mAh g^{-1} initial capacity at $C/20$ rate, but the rate performance is poor. The capacity at $1C$ rate is only 60 mAh g^{-1} (40% of theoretical capacity). In the case of the $LiFePO_4/Fe_2P$ composite, the initial capacity was slightly lower than that of pure $LiFePO_4$, however, 110 mAh g^{-1} (70% of the theoretical capacity) remained at $1C$ rate. Obviously we can see the presence of Fe_2P dramatically improves the rate performance.

4. Conclusions

The carbothermal reduction method with excess carbon was used to prepare 10% Mn substituted $LiFe_{0.9}Mn_{0.1}PO_4/Fe_2P$ composite materials. By using ball-milled precursors a short-time firing (i.e. 30 min) at higher temperature (i.e. 900 °C) was sufficient to prepare smaller sized but fully crystallized samples. The amount of conductive Fe_2P phase was fixed near to the optimum of 4% by modifying the carbon excess. The composite sample shows high electronic conductivity due to the presence of conductive Fe_2P. The diffusion coefficient was measured, confirming that 10% Mn

substitution enhances the Li ionic transport. Correspondingly, the 10% Mn substituted sample shows the best electrochemical performance at higher rate.

References

[1] A.K. Padhi, K.S. Nanjundaswamy, J.B. Goodenough, J. Electrochem. Soc. 144 (1997) 1188.
[2] A. Yamada, S. Chung, J. Electrochem. Soc. 148 (2001) A960.
[3] A.S. Andersson, B. Kalska, L. Häggström, J.O. Thomas, Solid State Ionics 133 (2000) 41.
[4] A.S. Andersson, J.O. Thomas, B. Kalska, L. Häggström, Electrochem. Solid State Lett. 3 (2000) 66.
[5] S.Y. Chung, J.T. Bloking, Y.M. Chiang, Nat. Mater. 1 (2002) 123.
[6] N. Terada, T. Yanagi, S. Arai, M. Yoshikawa, K. Ohta, N. Nakajima, N. Arai, J. Power Sources 1–2 (2001) 80–92.
[7] M.M. Doeff, Y. Hu, F. Mclarnon, R. Kostecki, Electrochem. Solid State Lett. 6 (2003) A207.
[8] Z. Chen, J.R. Dahn, J. Electrochem. Soc. 149 (2002) A1184.
[9] G.X. Wang, L. Yang, S.L. Bewlay, Y. Chen, H.K. Liu, J.H. Ahn, J. Power Sources 146 (2005) 521–524.
[10] S. Shi, L. Liu, C. Ouyang, D.S. Wang, Z. Wang, L. Chen, X. Huang, Phys. Rev. B 68 (2003) 195108.
[11] D. Wang, H. Li, S. Shi, X. Huang, L. Chen, Electrochem. Acta 50 (2005) 2955.
[12] G.X. Wang, S.L. Bewlay, K. Konstantinov, H.K. Liu, S.X. Dou, J.-H. Ahn, Electrochem. Acta 50 (2004) 443.
[13] M.R. Yang, W.H. Ke, S.H. Wu, J. Power Sources 165 (2007) 646.
[14] Y. Xia, M. Yoshio, H. Noguchi, Electrochim. Acta 52 (2006) 240–245.
[15] D. Choi, P.N. Kumta, J. Power Sources 163 (2007) 1064.
[16] Y. Wang, G.Z. Cao, Adv. Mater. 20 (2008) 2251.
[17] P.S. Herle, B. Ellis, N. Coombs, L.F. Nazar, Nat. Mater. 3 (2004) 147.
[18] J. Baker, M.Y. Saidi, J.L. Swoyer, Electrochem. Solid State Lett. 6 (2003) A53.
[19] C.H. Kim, J.S. Park, K.S. Lee, J. Power Sources 163 (2006) 144–150.
[20] Y. Xu, Y. Lu, L. Yan, Z. Yang, R. Yang, J. Power Sources 160 (2006) 570–576.
[21] C.H. Kim, M.H. Lee, W.T. Jeong, K.S. Lee, J. Power Sources 146 (2005) 534–538.
[22] P.P. Prosini, M. Lisi, D. Zane, M. Pasquali, Solid State Ionics 148 (2002) 45–51.
[23] W. Weppner, R.A. Huggins, J. Electrochem. Soc. 124 (1977) 1569.
[24] E. Deiss, Electrochim. Acta 50 (2005) 2927–2932.
[25] T. Nakamura, K. Sakumoto, M. Okamoto, S. Seki, Y. Kobayashi, T. Takeuchi, M. Tabuchi, Y. Yamada, J. Power Sources 174 (2007) 435–441.